25th ABCM International Congress of Mechanical Engineering
October 20-25, 2019, Uberlândia, MG, Brazil

COB-2019-0050
ROBUST H_∞ COMPUTED TORQUE CONTROL OF ROBOT MANIPULATORS

Fabian Andres Lara-Molina
Edson Hideki Koroishi
Federal University of Technology - Paraná, Mechanical Engineering Department, Av. Alberto Carazzai 1640, Cornélio Procópio-PR, Brazil
fabianmolina@utfpr.edu.br, edsonh@utfpr.edu.br

Aldemir Ap. Cavalini Jr
Valder Steffen Jr
LMEst - Structural Mechanics Laboratory, Federal University of Uberlândia, School of Mechanical Engineering, Av. João Naves de Ávila, 2121, Uberlândia, MG, 38408-196, Brazil
aacjunior@ufu.br

Abstract. *This paper proposes the synthesis and the application of a robust control technique in a manipulator. This control technique is based on LMIs (Linear Matrix Inequalities) to minimize the $\mathcal{H}_\infty$ norm by taking into account the uncertain parameters. The control strategy is based on the computed torque control scheme. The numerical results show the benefits of the robustified control strategy in the dynamical performance regarding tracking accuracy, disturbance rejection, and uncertain parameters.*

Keywords: *Robot control, Robust Control, Manipulator, Uncertainty, Computed Torque Control.*

1. INTRODUCTION

Robotic manipulations have been used on varius applications such as manufacture tasks, precision surgery, and pick-and-place operations. These applications demand the execution of specific motions with high accuracy and reliability. Nevertheless, several operational factors such as sensor noise, no-modeled dynamics, and uncertain parameters can decrease the performance of the robotic manipulators. The design of advanced control systems is an approach widely used to face this problem. Thus, the dynamic performance of robotic manipulators could be enhanced (Lara-Molina, 2012).

The control laws of robotic manipulators are based on their dynamic model. Therefore, the formulation of the dynamic model and the identification of their parameters are essential aspects in the design of controllers. However, the dynamic model is a simplified mathematic representation of the real dynamics. Thus, several dynamic effects can be neglected in the dynamic model and therefore, reducing the controller performance. Moreover, the parameter identification methods introduce errors associated with the identified parameters. In this context, two strategies have been widely applied: adaptative and robust control (Lewis *et al.*, 2003). Consequently, it is necessary to synthesize robust control laws in order to deal with non-modeled dynamics, uncertain parameters, and external disturbances.

In this direction, several research works have been developed aiming at robustifying the motion controllers. Mainly, five principal approaches have been applied for the robust control of robotic manipulators (Sage *et al.*, 1999): i) linear multivariable control, ii) passive controllers, iii) variable structure controllers, vi) saturation controllers v) adaptative robust controllers.

This contribution aims at presenting an alternative approach for the robust linear multivariable control. A computed torque law is robustified by using Linear Matrix Inequalities - LMIs that minimize the $\mathcal{H}_\infty$ norm (Chilali and Gahinet, 1996). The proposed control law permits the inclusion of uncertain parameters and non-modeled dynamics within a linear equivalent model used in the design of the controller. For this purpose, the parametric uncertainties are modeled as random variables, and the equivalent model considered in the design of the controller is obtained by using the Monte Carlo Simulation. It permits to determine the polytopic representation. This representation is introduced in the LMIs, and then the controller gains are achieved by minimizing the $\mathcal{H}_\infty$ norm.

2. DYNAMIC MODEL OF THE MANIPULATOR

The dynamic model can be obtained by using the Lagrange formulation (Lewis *et al.*, 2003). The dynamics of the joints and links for a serial manipulator with n joints is presented in the following equation:

$$\mathbf{M}(\boldsymbol{\theta})\ddot{\boldsymbol{\theta}} + \mathbf{v}(\boldsymbol{\theta}, \dot{\boldsymbol{\theta}}) + \mathbf{f}(\dot{\boldsymbol{\theta}}) + \mathbf{g}(\boldsymbol{\theta}) + \boldsymbol{\tau}_d = \boldsymbol{\tau} \tag{1}$$

where $\boldsymbol{\theta} \in \mathbb{R}^n$ is the vector of the joint position; $\dot{\boldsymbol{\theta}} \in \mathbb{R}^n$ is the velocity of the joints; $\ddot{\boldsymbol{\theta}} \in \mathbb{R}^n$ is the acceleration of the joints; $\mathbf{M}(\boldsymbol{\theta}) \in \mathbb{R}^{n\times n}$ is the inertia matrix; $\mathbf{v}(\boldsymbol{\theta}, \dot{\boldsymbol{\theta}}) \in \mathbb{R}^n$ are the forces and moments of Coriolis; $\mathbf{f}(\dot{\boldsymbol{\theta}}) \in \mathbb{R}^n$ is the joint friction; $\mathbf{g}(\boldsymbol{\theta}) \in \mathbb{R}^n$ is the gravitational forces; and, $\boldsymbol{\tau}_d \in \mathbb{R}^n$ is the disturbance moment in the joints. The dynamic equation of Eq. (1) can be rewrite in a simplified form considered that $\mathbf{h}(\boldsymbol{\theta}, \dot{\boldsymbol{\theta}}) = \mathbf{v}(\boldsymbol{\theta}, \dot{\boldsymbol{\theta}}) + \mathbf{f}(\dot{\boldsymbol{\theta}}) + \mathbf{g}(\boldsymbol{\theta})$, thus:

$$\mathbf{M}(\boldsymbol{\theta})\ddot{\boldsymbol{\theta}} + \mathbf{h}(\boldsymbol{\theta}, \dot{\boldsymbol{\theta}}) + \boldsymbol{\tau}_d = \boldsymbol{\tau} \tag{2}$$

3. COMPUTED TORQUE CONTROL WITH UNCERTAINTIES

3.1 Computed Torque Control

The computed torque is applied to the feedback linearization of non-linear systems, as presented by (Hunt *et al.*, 1983). Moreover, the computed torque control has been used together with robust control techniques in the position control (Lara-Molina *et al.*, 2014). The scheme of the computed torque control (see Fig. 1) is composed of two independent control loops: an inner loop which linearizes the dynamics of the manipulator and an outer loop which tracks the set-point trajectory. In the inner loop, the parameters of the dynamic equation (of Eq. (2)) should be identified to compute the control law. Therefore, the terms of the dynamic equation considering the identified parameters $\hat{\mathbf{M}}(\boldsymbol{\theta})\ddot{\boldsymbol{\theta}}$ and $\hat{\mathbf{h}}(\boldsymbol{\theta}, \dot{\boldsymbol{\theta}})$ are defined based on the Eq. (2). Initially, it is assumed that the identified parameters are equal to the parameters of the manipulator, thus $\hat{\mathbf{M}}(\boldsymbol{\theta}) = \mathbf{M}(\boldsymbol{\theta})$ and $\hat{\mathbf{h}}(\boldsymbol{\theta}, \dot{\boldsymbol{\theta}}) = \mathbf{h}(\boldsymbol{\theta}, \dot{\boldsymbol{\theta}})$. Moreover, non-modeled dynamics and noise sensors are neglected. The set-point trajectory in the jointspace is completely defined by the jont position, velocity, and aceleration.

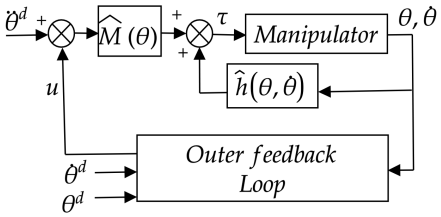

Figure 1. Computed Torque Control diagram.

Thus: $\boldsymbol{\theta}^d(t)$, $\dot{\boldsymbol{\theta}}^d(t)$ and $\ddot{\boldsymbol{\theta}}^d(t)$. Consequently, the position, velocity, and acceleration errors ($\mathbf{e}$, $\dot{\mathbf{e}}$ and $\ddot{\mathbf{e}}$, respectively) are defined as:

$$\mathbf{e} = \boldsymbol{\theta}^d - \boldsymbol{\theta}, \qquad \dot{\mathbf{e}} = \dot{\boldsymbol{\theta}}^d - \dot{\boldsymbol{\theta}}, \qquad \ddot{\mathbf{e}} = \ddot{\boldsymbol{\theta}}^d - \ddot{\boldsymbol{\theta}} \tag{3}$$

Considering the Eq. (2) with the identified parameters and solving for $\ddot{\boldsymbol{\theta}}$, it is obtained: $\ddot{\boldsymbol{\theta}} = \hat{\mathbf{M}}^{-1}[\boldsymbol{\tau} - \boldsymbol{\tau}_d - \hat{\mathbf{h}}]$. Moreover, by substituing $\ddot{\mathbf{e}}$ in Eq. (3), it is obtained:

$$\ddot{\mathbf{e}} = \ddot{\boldsymbol{\theta}}^d + \hat{\mathbf{M}}^{-1}[\hat{\mathbf{h}} - \boldsymbol{\tau} - \boldsymbol{\tau}_d] \tag{4}$$

The input control and the disturbances are defined as $\mathbf{u}$ and $\mathbf{w}$, respectively. Thus:

$$\mathbf{u} = \ddot{\boldsymbol{\theta}}^d + \hat{\mathbf{M}}^{-1}[\hat{\mathbf{h}} - \boldsymbol{\tau}] \tag{5}$$

$$\mathbf{w} = \hat{\mathbf{M}}^{-1}\boldsymbol{\tau}_d \tag{6}$$

The state space representation of the error dynamics (of Eq. (4)) is defined based on the equations presented previously. The state space vector $x = \begin{bmatrix}\mathbf{e} & \dot{\mathbf{e}}\end{bmatrix}^T$, with $x \in \mathbb{R}^{2n}$, thus:

$$\frac{d}{dt}\begin{bmatrix}\mathbf{e}\\ \dot{\mathbf{e}}\end{bmatrix} = \begin{bmatrix}0 & \mathbf{I}_n\\ 0 & 0\end{bmatrix}\begin{bmatrix}\mathbf{e}\\ \dot{\mathbf{e}}\end{bmatrix} + \begin{bmatrix}0\\ \mathbf{I}_n\end{bmatrix}\mathbf{u} + \begin{bmatrix}0\\ \mathbf{I}_n\end{bmatrix}\mathbf{w} \tag{7}$$

The compute torque control law is defined based on the dynamic model of the Eq. (2) considering the idetified terms,5 thus

$$\boldsymbol{\tau} = \hat{\mathbf{M}}\ddot{\boldsymbol{\theta}} + \hat{\mathbf{h}} + \boldsymbol{\tau}_d \tag{8}$$

The non-linear transformation of the Eq. (5) states a non-linear controller design into a linear and joint decoupled design controller. It is worth to mention that control law depends on the inversion of the dynamic equation. Thus, $\boldsymbol{\tau}$ can be computed using the Eq. (2). Robust linear control techniques can calculate the control input control. It is worth to mention that the computed torque control law depends on the inversion of the dynamic equation of the manipulator, thus $\boldsymbol{\tau}$ can be computed using the Eq. (2), and substituting $\ddot{\boldsymbol{\theta}}$ by $\boldsymbol{\theta}^d - \mathbf{u}$. The control of the outer feedback loop can be computed through linear control techniques such as robust linear control approaches.

3.2 Computed Torque with Uncertainties

The structure of the computed control with uncertainties has been considered in the literature as a non-linear disturbance applied to the linear model of the position error dynamics presented in the Eq. (7) (Lewis *et al.*, 2003; Spong, 1992; Qu and Dawson, 1995), thus:

$$\begin{aligned} \dot{\mathbf{e}} &= \mathbf{A}\mathbf{e} + \mathbf{B}(\mathbf{u} + \boldsymbol{\upsilon}) \\ \boldsymbol{\upsilon} &= \boldsymbol{\Delta}(\mathbf{u} - \ddot{\boldsymbol{\theta}}^d) + \mathbf{M}^{-1}\boldsymbol{\delta} \\ \boldsymbol{\Delta} &= \mathbf{M}^{-1}\hat{\mathbf{M}} - \mathbf{I}_n, \quad \boldsymbol{\delta} = \mathbf{h} - \hat{\mathbf{h}} \end{aligned} \tag{9}$$

Nevertheless, the formulation presented previously in the Eq. (9) takes into account the uncertainties as the non-linear input $\boldsymbol{\upsilon}$. This approach gets difficult to quantify the effect of the uncertainties in the computed torque control, and therefore, the design of the controller using linear control techniques. However, several authors have presented several approaches by using this approach (Sage *et al.*, 1999). The present contribution proposes an alternative to this approach that consists of obtaining a linear model, including the uncertain parameters within the Eq. (7).

The dynamic equation of the manipulator, presented in the Eq. (2) and the computed torque control law showed in the Eq. (8) are using with a modification that consists in substituing $\ddot{\boldsymbol{\theta}}$ by $\hat{\mathbf{M}}^{-1}\mathbf{M}\ddot{\boldsymbol{\theta}}^d - \mathbf{u}$, thus:

$$\boldsymbol{\tau} = \hat{\mathbf{M}}\left(\hat{\mathbf{M}}^{-1}\mathbf{M}\ddot{\boldsymbol{\theta}}^d - \mathbf{u}\right) + \hat{\mathbf{h}} \tag{10}$$

Using the Eqs. (2) and (10) thogheter with the definition of the tracking error of the Eq. (3), it is obtained an expression that defines completaly the dynamic of the tracking error that considers the identified parameters in $\hat{\mathbf{M}}$ and $\hat{\mathbf{h}}$, thus:

$$\ddot{\mathbf{e}} = \mathbf{M}^{-1}\hat{\mathbf{M}}\mathbf{u} + \mathbf{M}^{-1}\left(\mathbf{h} - \hat{\mathbf{h}}\right) + \mathbf{M}^{-1}\boldsymbol{\tau}_d \tag{11}$$

It is worth to mention that the identified parameters of the terms $\hat{\mathbf{M}}$ and $\hat{\mathbf{h}}$ introduce uncertainties on the systems, i.e., there are small differences between the identified terms in $\mathbf{M}$ and $\mathbf{h}$. The space state representation for the dynamics of the error of the Eq. (11) is presented as follows:

$$\frac{d}{dt}\begin{bmatrix}\mathbf{e}\\ \dot{\mathbf{e}}\end{bmatrix} = \begin{bmatrix}0 & \mathbf{I}_n\\ 0 & 0\end{bmatrix}\begin{bmatrix}\mathbf{e}\\ \dot{\mathbf{e}}\end{bmatrix} + \begin{bmatrix}0\\ \mathbf{M}^{-1}\hat{\mathbf{M}}\end{bmatrix}\mathbf{u} + \begin{bmatrix}0\\ \mathbf{M}^{-1}\left(\mathbf{h} - \hat{\mathbf{h}}\right)\end{bmatrix} + \begin{bmatrix}0\\ \mathbf{M}^{-1}\end{bmatrix}\mathbf{w} \tag{12}$$

Consequently, by using the auxiliar variables $\boldsymbol{\eta} = \mathbf{M}^{-1}\hat{\mathbf{M}}$ and $\boldsymbol{\lambda} = \mathbf{M}^{-1}\left(\mathbf{h} - \hat{\mathbf{h}}\right)$, it is obtained:

$$\frac{d}{dt}\begin{bmatrix}\mathbf{e}\\ \dot{\mathbf{e}}\end{bmatrix} = \begin{bmatrix}0 & \mathbf{I}_n\\ 0 & 0\end{bmatrix}\begin{bmatrix}\mathbf{e}\\ \dot{\mathbf{e}}\end{bmatrix} + \begin{bmatrix}0\\ \boldsymbol{\eta}\end{bmatrix}\mathbf{u} + \begin{bmatrix}0\\ \boldsymbol{\lambda}\end{bmatrix} + \begin{bmatrix}0\\ \boldsymbol{\phi}\end{bmatrix}\mathbf{w} \tag{13}$$

or

$$\begin{aligned} \dot{\mathbf{e}} &= \mathbf{A}\mathbf{e} + \mathbf{B}\mathbf{u} + \boldsymbol{\Lambda} + \mathbf{B}_1\mathbf{w} \\ \mathbf{y} &= \mathbf{C}\mathbf{e} + \mathbf{D}\mathbf{u} + \mathbf{D}_1\mathbf{w} \end{aligned} \tag{14}$$

with $\mathbf{C} = \mathbf{I}_n$, $\mathbf{D} = \mathbf{D}_1 = \mathbf{0}_n$ and $\boldsymbol{\Lambda} = \begin{bmatrix}0 & \boldsymbol{\lambda}\end{bmatrix}^T$; $\boldsymbol{\Lambda}$ is also an exogen input in the system. The Eq. (13) shows that the uncertainties in the inertial parameters introduce a coupling between the joints, and they apply disturbances in the system. Therefore, the expression showed in the Eq. (14) shows a linear model for the computed torque with uncertainties as an alternative to the model previously showed in the Eq. (9).

4. Modeling and Quantification of the Uncertainties

The Monte Carlo Simulation is a numerical method that permits quantify the effect of uncertainties in a numerical model, and it can be applied to the linear model with uncertain parameters presented in the Eqs. (12) e (14).

Correctly, the uncertain parameters are modeled as random variables; this particular model fits the results obtained from the parameter identification procedure (Lara-Molina *et al.*, 2015). The non-modeled dynamics mainly produce the error associated with the standard deviation of the identified parameters, sensors noise, and variations on the operational conditions (Wu *et al.*, 2010).

4.1 Modeling of Uncertain Parameters

The uncertain parameters as modeled as uncertain parameters because of their mathematical representation permits to associate the identification results for each identified parameters by using the last square methods. Therefore, the uncertain parameters are modeled as follows:

$$\hat{k}_i(\Omega) = \hat{k}_i + \hat{k}_i \sigma_i \xi(\Omega) \tag{15}$$

where for each parameter $\hat{k}_i$ is the mean, σ_i is the maximum percentual standard deviation and $\xi(\Omega)$ is a normal random variable with Ω is a stochastic process. The normal random variable is gorverned by a normal probability density function.

4.2 Monte Carlo Simulation

The Monte Carlo simulation combined with the Latin Hypercube method permits to sample the random variables to evaluate the effects on the uncertain parameters in the model; additional details about the computation implementation of the method can be found in (Florian, 1992). Consequently, the maximum and minimum values of the coefficients of the model presented in the Eq. (14), thus:

$$\begin{aligned} \dot{\mathbf{e}} &= \mathbf{A}\mathbf{e} + \max \mathbf{B}(\Omega)\mathbf{u} + \max \mathbf{\Lambda}(\Omega) + \max \mathbf{B}_1(\Omega)\mathbf{w} \\ \mathbf{y} &= \mathbf{C}\mathbf{e} + \mathbf{D}\mathbf{u} + \mathbf{D}_1\mathbf{w} \end{aligned} \tag{16}$$

and

$$\begin{aligned} \dot{\mathbf{e}} &= \mathbf{A}\mathbf{e} + \min \mathbf{B}(\Omega)\mathbf{u} + \min \mathbf{\Lambda}(\Omega) + \min \mathbf{B}_1(\Omega)\mathbf{w} \\ \mathbf{y} &= \mathbf{C}\mathbf{e} + \mathbf{D}\mathbf{u} + \mathbf{D}_1\mathbf{w} \end{aligned} \tag{17}$$

The formulation presented in the Eqs. (16) and (17) permits the project of the control law for the external feedback loop of the Fig. 1.

5. Robust Control for the External Feedback Loop

The robust controller is based on LMIs to minimize the $\mathcal{H}_\infty$ cost (Chilali and Gahinet, 1996); this procedure permits to include the uncertainties in the computed torque for the tracking position control. The design of the external feedback loop system will be performed using a proportional and derivative controller in which the states are feedbacked. Therefore, the control $\mathbf{u}$, of the Fig. 1 consists of:

$$\mathbf{u} = \mathbf{K}\mathbf{e} \tag{18}$$

with $\mathbf{K} \in \mathbb{R}^{n \times 2n}$ being the gain matrix of the controller.

5.1 $\mathcal{H}_\infty$ Control with polytopic uncertainties

The uncertainties of a system can be divided into two main groups: parametric uncertainties and uncertainties produced by the non-modeled dynamic. The uncertainties parameters refer to small variations in system parameters.

In the controller design, dynamic matrices are represented by polytopic modeling. A polytope is the smallest convex shell that contains all the vertices of a finite set. Moreover, every element in the polytope can be written as a convex combination of vertices (Aguirre *et al.*, 2007). Then, be a polytope P with $kappa$ vertices, any point p that belongs to the polytope can be written as:

$$p = \sum_{i=1}^{\kappa} \beta_i \kappa_i \tag{19}$$

sendo:

$$\begin{array}{c} \beta_i \geq 0; \\ \sum_{i=1}^{\kappa} \beta_i = 1 \end{array} \tag{20}$$

Considering the model of the manipulator of the Eq. (14), wiht $\mathbf{\Lambda} << \mathbf{B_1 w}$, the uncertanties can be parametrized as follows:

$$\begin{array}{rcl} \dot{\mathbf{x}} & = & \mathbf{A}(\beta)\mathbf{x} + \mathbf{B}(\beta)\mathbf{u} + \mathbf{B}_1(\beta)\mathbf{w} \\ \mathbf{y}(t) & = & \mathbf{C}(\beta)\mathbf{x} + \mathbf{D}(\beta)\mathbf{u} + \mathbf{D}_1(\beta)\mathbf{w} \end{array} \tag{21}$$

being:

$$\begin{aligned} \mathbf{A}(\beta) &= \sum_{i=1}^{\kappa} \beta_i \mathbf{A_i}, \quad \mathbf{C}(\beta) = \sum_{i=1}^{\kappa} \beta_i \mathbf{C_i} \\ \mathbf{B}(\beta) &= \sum_{i=1}^{\kappa} \beta_i \mathbf{B_i}, \quad \mathbf{B_1}(\beta) = \sum_{i=1}^{\kappa} \beta_i \mathbf{B_{1i}} \\ \mathbf{D}(\beta) &= \sum_{i=1}^{\kappa} \beta_i \mathbf{D_i}, \quad \mathbf{D_1}(\beta) = \sum_{i=1}^{\kappa} \beta_i \mathbf{D_{1i}} \\ \Lambda_\kappa &= \{\beta \in \mathbb{R}^m \kappa : \sum_{i=1}^{\kappa} \beta_i = 1, \beta_i \geq 0\} \end{aligned} \tag{22}$$

being $(\mathbf{A_i}, \mathbf{B_i}, \mathbf{B_{1i}}, \mathbf{C_i}, \mathbf{D_i}, \mathbf{D_{1i}})$ the vertices of the polytope and $mathbfx$ the state vector of the system. Based on the representation of the system showed in the Eq. (21), it is design a robust control $\mathcal{H}_\infty$ with polytopic uncertainties and non-modeled dynamics. The norm $\mathcal{H}_\infty$ corresponds to the greatest amplification factor of the steady-state response to a sinusoidal excitation (Zhou *et al.*, 1996). Then, in order to minimize the effects caused by the unmodified dynamics or exogenous input $\mathbf{w}$ in the output $\mathbf{y}$ of the system, minimizes the standard $\mathcal{H}_\infty$ (Manesco and P., 2012).

Considering taht $G(s)$ is the output function of the system $\mathbf{y}$, and the exogen input $\mathbf{w}$, being $s = j\omega$ the Laplace variable, the norm $\mathcal{H}_\infty$ of $G(s)$ is defined as:

$$\|G(s)\|_\infty = \Phi_{max}[G(j\omega)] \tag{23}$$

being Φ_{max} the maximum singular value of $G(j\omega)$. The magnitude of $G(s)$ is limited by γ, thus:

$$\|G(s)\|_\infty < \gamma \tag{24}$$

In this way, with the purpose of the magnitude of $\|G\|_\infty$ will be reduced, γ is minimized. Therefore, by minimizing the $\mathcal{H}_\infty$ norm of $G(s)$, the effects produced by the non-modeled dynamics, $\mathbf{w}$, are also minimized in the output of the system. Then, the norm $\mathcal{H}_\infty$ of the system of the Eq. (21), which transfer function is $G(s)$ can be characterized as (Manesco and P., 2012):

$$\|G(s)\|_\infty \leq \gamma \Leftrightarrow \mathbf{y}^T\mathbf{y} < \gamma^2 \mathbf{w}^T\mathbf{w} \tag{25}$$

Consequently, the Eq. (25) is written again, thus:

$$\mathbf{y}^T\mathbf{y} - \gamma^2 \mathbf{w}^T\mathbf{w} < 0 \tag{26}$$

The system stability of the Eq. (26) must be verified to calculate the norm $\mathcal{H}_\infty$. Therefore, the Lyapunov candidate function to evaluate the stability of the system is presented in the equation (27). The stability is checked if its derivative $\dot{\mathbf{V}}(\mathbf{x})$ is defined negative and considering the equation (26), thus:

$$\mathbf{V}(\mathbf{x}) = \mathbf{x}^T\mathbf{P}\mathbf{x}, \quad \mathbf{P} = \mathbf{P}^T \tag{27}$$

with:

$$\dot{\mathbf{V}}(\mathbf{x}) = \dot{\mathbf{x}}^T\mathbf{P}\mathbf{x} + \mathbf{x}^T\mathbf{P}\dot{\mathbf{x}} < 0 \tag{28}$$

From the Eqs. (26) and (28):

$$\dot{\mathbf{V}}(\mathbf{x}) + \mathbf{y}^T\mathbf{y} - \gamma^2 \mathbf{w}^T\mathbf{w} < 0 \tag{29}$$

Equation (29) is rewritten, thus:

$$\dot{\mathbf{x}}^T\mathbf{P}\mathbf{x} + \mathbf{x}^T\mathbf{P}\dot{\mathbf{x}} + \mathbf{y}^T\mathbf{y} - \gamma^2\mathbf{w}^T\mathbf{w} < 0 \tag{30}$$

On the other hand the closed loop system is obtained considering the law of control of the Eq. (18) and the system of the Eq. (21):

$$\begin{aligned}\dot{\mathbf{x}} &= \mathbf{A}_{cl}(\beta)\mathbf{x} + \mathbf{B}_1(\beta)\mathbf{w}\\ \mathbf{y} &= \mathbf{C}_{cl}(\beta)\mathbf{x} + \mathbf{D}_1(\beta)\mathbf{w}\end{aligned} \tag{31}$$

with:

$$\begin{aligned}\mathbf{A_{cl}}(\beta) &= \mathbf{A}(\beta) - \mathbf{B}(\beta)\mathbf{K}\\ \mathbf{C_{cl}}(\beta) &= \mathbf{C}(\beta) - \mathbf{D}(\beta)\mathbf{K}\end{aligned}$$

Substituting the Eq. (31) in the Eq. (30) and performig additional mathematical manipulalations, the non-linear matrix inequality is obtained:

$$\begin{bmatrix}\mathbf{S}_1 & \mathbf{S}_2\\ \mathbf{S}_2^T & \mathbf{S}_3\end{bmatrix} < 0 \tag{32}$$

where, $\mathbf{S}_1 = \mathbf{A_{cl}}^T(\beta)\mathbf{P} + \mathbf{P}\mathbf{A}_{cl}(\beta) + \mathbf{C}_{cl}^T(\beta)\mathbf{C}_{cl}(\beta)$, $\mathbf{S}_2 = \mathbf{P}\mathbf{B}_1(\beta) + \mathbf{C}_{cl}^T(\beta)\mathbf{D}_1(\beta)$, $\mathbf{S}_3 = \mathbf{D}_1^T(\beta)\mathbf{D}_1(\beta) - \gamma^2\mathbf{I}$. Defining that $\mathbf{W} = \mathbf{P}^{-1}$ and $\mathbf{Z} = \mathbf{K}\mathbf{W}$, and pre-multiplying and post-multiplying the Eq. (32), respectively, by:

$$\begin{bmatrix}\mathbf{P}^{-1} & 0\\ 0 & \mathbf{I}\end{bmatrix}^{-1} \qquad \begin{bmatrix}\mathbf{P}^{-1} & 0\\ 0 & \mathbf{I}\end{bmatrix}^{-T} \tag{33}$$

Thus, it is obtained:

$$\begin{bmatrix} Q_1 & Q_2\\ Q_2^T & Q_3\end{bmatrix} < 0 \tag{34}$$

with:
$Q_1 = \mathbf{A}(\beta)\mathbf{X} + \mathbf{X}\mathbf{A}^T(\beta) + \mathbf{B_2}(\beta)\mathbf{G} + \mathbf{G}^T\mathbf{B}_2^T(\beta) + (\mathbf{X}\mathbf{C}^T(\beta) + \mathbf{G}^T\mathbf{D_2}^T(\beta))(\mathbf{C}(\beta)\mathbf{X} + \mathbf{D_2}(\beta)\mathbf{G})$;
$Q_2 = \mathbf{B_1}(\beta) + (\mathbf{X}\mathbf{C}^T(\beta) + \mathbf{G}^T\mathbf{D_2}^T(\beta))\mathbf{D_1}(\beta)$;
$Q_3 = \mathbf{D_1}^T(\beta)\mathbf{D_1}(\beta) - \gamma\mathbf{I}$.

Thus, by applying the Schur complement in the Eq. (34) that transforms the nonlinear matrix inequalities into LMIs (Assunção and Teixeira, 2001) and making $\mu = \gamma^2$, the system of the Eq. (21) is stabilized by the control law of Eq. (18) if the matrices $\mathbf{Z}$, $\mathbf{W} = \mathbf{W}^T$ are feasible in the optimization problem:

$$\begin{aligned}\min\quad & \mu\\ & \mathbf{Z}, \mathbf{W} = \mathbf{W}^T > 0\\ s.a.\quad & \\ & \begin{bmatrix}\mathbf{Q} & \mathbf{B_{1i}} & \mathbf{W}\mathbf{C}_i^T + \mathbf{Z}^T\mathbf{D_{2i}}^T\\ * & -\mu\mathbf{I} & \mathbf{D_{1i}}\\ * & * & -\mathbf{I}\end{bmatrix} < 0\end{aligned} \tag{35}$$

with: $Q = \mathbf{A}_i\mathbf{W} + \mathbf{W}\mathbf{A}_i^T + \mathbf{B}_i\mathbf{Z} + \mathbf{Z}^T\mathbf{B}_i^T$.

Therefore, we can minimize $\|H\|_\infty$ by solving the problem of optimizing the Eq. (35) (Manesco and P., 2012). Additionally, the feedback gain matrix of the control law of the Eq. (18) is given by:

$$\mathbf{K} = \mathbf{Z}\mathbf{W}^{-1} \tag{36}$$

For symmetric matrices of Eq. (35) are assumed to have appropriate dimensions. The symbol $(*)$ indicates the term transposed in the matrix.

6. Case Study

The proposed methodology was applied to the tracking position control of a two planar (RR) manipulator showed in Fig. 2, i.e., a manipulator with two revolute joints. The identified parameters of the manipulator are presented in Tab. 1. The dynamic modeling and the controllers were implemented and numerically evaluated in Matlab/Simulink platform.

Figure 2. Planar Manipulator of two degrees of freedom (RR).

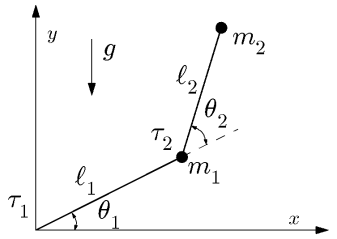

Table 1. Identified Parameters.

Parameter	$\hat{k}$	$\sigma(\%)$
$m_1[kg]$	0,2504	0,0653
c_1 [Nm]	0,9785	0,2602
v_1 [Nms/rad]	1,0034	0,0455
m_2 [kg]	0,2498	0,0291
c_2 [Nm]	0,9869	0,2611
v_2 [Nms/rad]	1,0018	0,0385

Table 2. Maximum and Minimum of $\boldsymbol{\eta}$.

Parameter	$\min \eta_{ij}$	$\max \eta_{ij}$
η_{11}	0.9994	1.0006
η_{12}	0.0000	0.0000
η_{21}	-0.0018	0.0016
η_{22}	0.9997	1.0003

Table 3. Maximum and Minimum of $\boldsymbol{\lambda}$.

Parameter	$\min \lambda_i$	$\max \lambda_i$
λ_1	-0.0007216	0.0007216
λ_2	-0.0001768	0.0001768

Table 4. Maximum and Minimum of $\boldsymbol{\phi}$.

Parameter	$\min \phi_{ij}$	$\max \phi_{ij}$
ϕ_{11}	32.0	64
ϕ_{12}	-128	0
ϕ_{21}	-128	0
ϕ_{22}	64	320

6.1 Implementation of $\mathcal{H}_\infty$ control

The parameters of the manipulator were identified previously by using the least-squares method (Costa *et al.*, 2016) (See Tab. 1). The identified parameters are characterized by the mean, $\hat{k}$, and the percentual standard deviation, σ. Additionally, ℓ_1 =0.2500m, ℓ_2 =0.2500m, and g =9.81m/s^2.

The limits considered in the evaluation of the joint limits are: 0$\leq \dot{\theta}_{1,2} \leq \pi$rad and -1rad/s$\leq \dot{\theta}_{1,2} \leq$-1rad/s. Consequently,the Monte Carlo Simulation Method permits to obtain the maximum and minimum values of the matrizes $\boldsymbol{\eta}$ and $\boldsymbol{\phi}$, and the vector $\boldsymbol{\lambda}$ (values showed in tabs. 2, 3 and 4). These values correspond to the polytope vertices. Based on tabs. 2, 3 and 4, the vertices of polytope are descrives as:

$$\mathbf{B}_1 = \begin{bmatrix} 0 & 0 \\ 0 & 0 \\ 1.0006 & 0.0000 \\ 0.0016 & 1.0003 \end{bmatrix} \quad \mathbf{B}_{11} = \begin{bmatrix} 0 & 0 \\ 0 & 0 \\ 64 & 0 \\ 0 & 320 \end{bmatrix} \quad \mathbf{\Lambda}_1 = \begin{bmatrix} 0 \\ 0 \\ 0.0007207 \\ 0.0001768 \end{bmatrix} \tag{37}$$

$$\mathbf{B}_2 = \begin{bmatrix} 0 & 0 \\ 0 & 0 \\ 0.9994 & 0.0000 \\ -0.0016 & 0.9997 \end{bmatrix} \quad \mathbf{B}_{12} = \begin{bmatrix} 0 & 0 \\ 0 & 0 \\ 32 & -128 \\ -128 & 64 \end{bmatrix} \quad \mathbf{\Lambda}_2 = \begin{bmatrix} 0 \\ 0 \\ -0.0007207 \\ -0.0001768 \end{bmatrix} \tag{38}$$

The outer control-loop is designed by solving the convex optimization problem using the YALMIP toolbox (*Yet Another LMI Parser*) in the Matlab software (Lofberg, 2005).

Therefore, the obtained control matrix is:

$$\mathbf{K} = \begin{bmatrix} 115.9557 & -60.8995 & 46.6925 & -25.0189 \\ 54.4661 & 275.7196 & 22.9276 & 111.5929 \end{bmatrix} \tag{39}$$

Additionally, a PD controller for the compute torque control without considering uncertainties as shown in the Eq. (7) was designed to evaluate the performance of the robust controller. For this case, the control matrix is: $\mathbf{K} = \begin{bmatrix} k_{p1} & 0 & k_{d1} & 0 \\ 0 & k_{p2} & 0 & k_{d2} \end{bmatrix}$. With $k_{pi} = \omega_n^2$ and $k_{di} = 2\xi\omega_n$, for $i = 1, 2$. This method of synthesis was widely used in the literature (Lewis *et al.*, 2003). By setting ξ =1 and ω_n =1.8rad/s, an equivalent reponse in the time domain was obtained using $\mathcal{H}_\infty$ controller approach. Thus, k_{pi} =3.24 and k_{di} =3.60 are obtained.

6.2 Numerical Results

Figures 3(a) and 3(b) shows the joints position for a step input with initial and final position $\theta_i^d = \begin{bmatrix} 0 & 0 \end{bmatrix}^T$ and $\theta_f^d = \begin{bmatrix} \pi/60 & \pi/36 \end{bmatrix}^T$, respectively. The results indicates that the setting time of the PD and $\mathcal{H}_\infty$ are equivalent. Nevertheless, one can see that the transient response with $\mathcal{H}_\infty$ controller is the fastest.

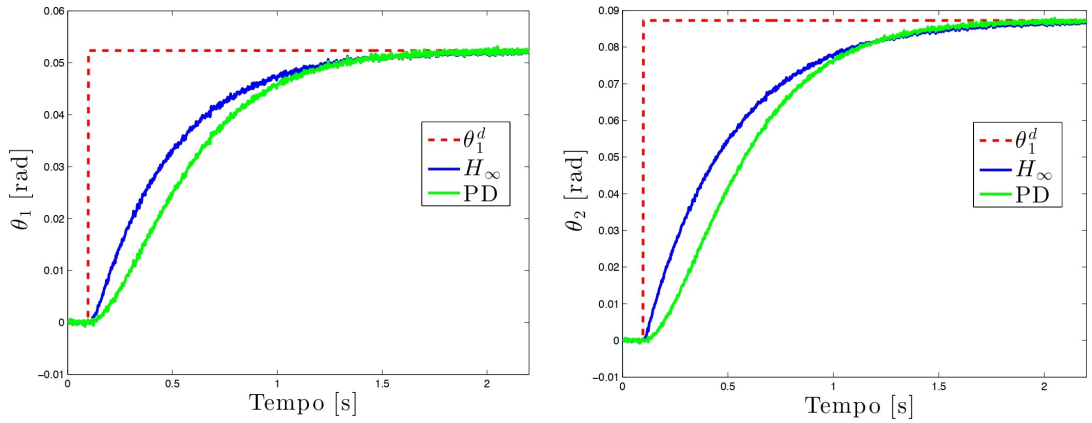

(a) Joint 1 position: θ_1. (b) Joint 2 position: θ_2.

Figure 3. Step response of the joints.

The figure 4(a) shows the end effector's circular reference tajectory in the workspace. Also, the trajectories tracked by the manipulator are presented with the $\mathcal{H}_\infty$ and the PD controllers. The results indicate that the tracking error is less using the $\mathcal{H}_\infty$ controller.

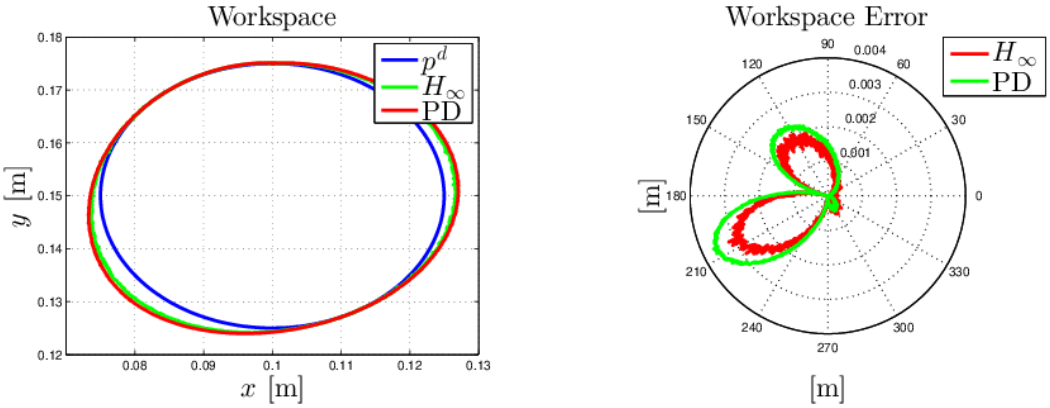

(a) Workspace circular trajectory. (b) Workspace tracking position error.

Figure 4. Circular workspace trajectory.

The figure 4(b) shows a polar representation of the tracking error in the workspace for the reference circular path of Fig. 4(a). Similarly, the results obtained in the jointspace, the tracking error in the workspace is smaller using the $\mathcal{H}_\infty$ controller. However, it is observed that the incidence of noise in the sensors is greater with the controller $\mathcal{H}_\infty$.

In this simulation, the manipulator rests fully extended in position $\theta = \begin{bmatrix} 0 & 0 \end{bmatrix}^T$; after 0.1s it is applied a disturbance torque $\tau = \begin{bmatrix} 1 & 1 \end{bmatrix}^T$Nm. As Figs. 5(a) and 5(b) show the the jointspace error. The results show that the effect of the disturbance torque with the $\mathcal{H}_\infty$ controller is much lower than the error in the joints being smaller using PD controller.

The figures 6(a) and 6(b) show the torques applied at the joints. Although the error produced by the disturbance is smaller using the control $\mathcal{H}_\infty$ the torque is also smaller in comparison to the one obtained with the contrador PD; this is due to the robustness characteristics of the non-modeled dynamics. In addition, the same behavior described above is observed by the coulomb friction for the torque at the joints when the manipulator is at rest.

Finally, Figs. 7(a) and 7(b) present the position of the joints for the step input with uncertainties in the inertial parameters using the Monte Carlo Simulation. Thus, m_1 and m_2 has a variation of 1% around the mean and the results present 20 samples.

It is observed for the two joints that small uncertainties in the parameters produce great errors for the position control deteriorating the precision in trajectory tracking using the PD controller. However, the results indicate that the controller $\mathcal{H}_\infty$ is less sensitive to the variation in the inertial parameters because the dispersion of the position of the first and second

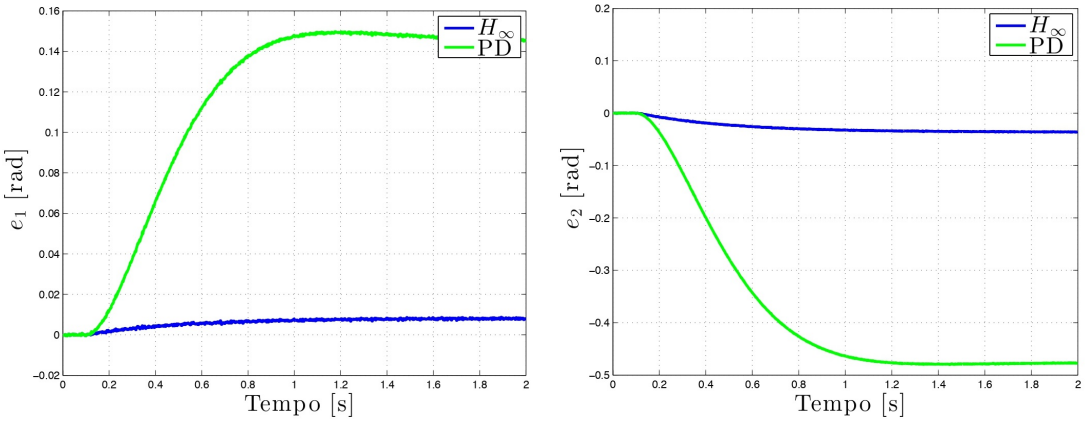

(a) Joint error 1: e_1. (b) Joint error 2: e_2.

Figure 5. Disturbance rejection test: joint error.

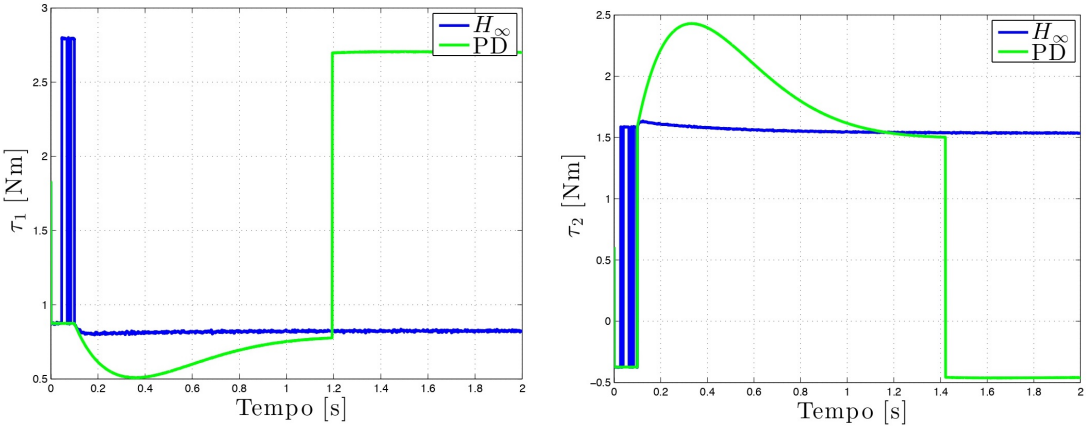

(a) Torque in the joint 1: τ_1. (b) Torque in the joint 2: τ_2.

Figure 6. Disturbance rejection test: joint torque.

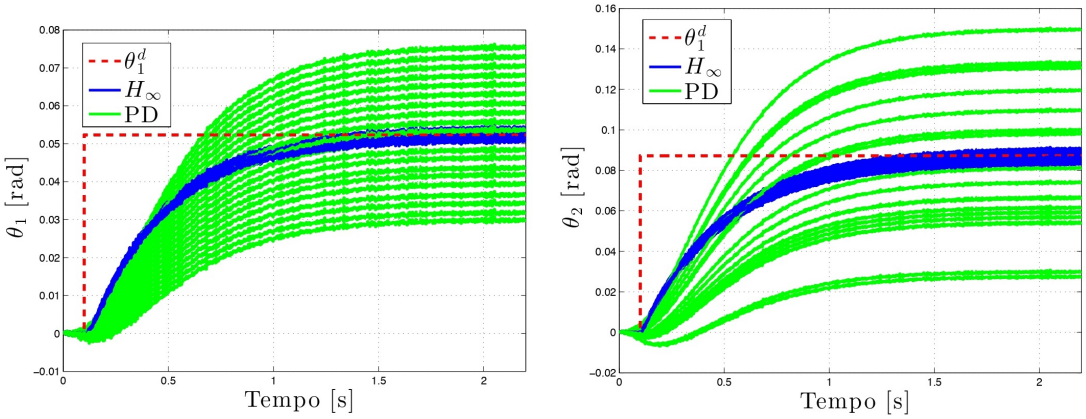

(a) Position of joint 1: θ_1. (b) Position of joint 2: θ_2.

Figure 7. Disturbance rejection test: joint torque.

joint is smaller with this controller. Therefore position errors are also reduced because of the robustness to parametric uncertainties.

7. CONCLUSIONS

This work proposed the design of a robust position control considering uncertain parameters in the manipulator. Consequently, the uncertain parameters were modeled as random variables; moreover, the nonmodeled dynamics were also considered in the model to design the control. The robust control is obtained by minimizing the $\mathcal{H}_\infty$ norm.

The numerical results obtained from the numerical simulations indicate that the robust controller design procedure proposed in this contribution minimize the effect of the uncertain parameters and non modeled dynamics that were considered as external disturbances. Therefore, the robust controller contributes to enhancing the dynamic performance of the manipulator. Future works aim at robust design of controllers applied on manipulators with flexible elements such as flexible joint and links.

8. ACKNOWLEDGEMENTS

The authors express their acknowledgements to the Graduate Program in Mechanical Engineering of the Federal University of Technology - Paraná funded by CAPES. The authors are also thankful for the financial support provided to the present research effort by CNPq (574001/2008-5, 304546/2018-8 and 427204/2018-6) and FAPEMIG (TEC-APQ-3076-09 and TEC-APQ-00464-16) through the INCT-EIE.

9. REFERENCES

Aguirre, L.A., Bruciapaglia, A.H., Miyagi, P.E. and Piqueira, J.R.C., 2007. *Enciclopédia de automática: controle e automação*. Blucher.

Assunção, E. and Teixeira, M.C., 2001. "Projeto de sistemas de controle via LMIs usando o MATLAB". *Aplicações em Dinâmica e Controle, São Carlos*, pp. 350–368.

Chilali, M. and Gahinet, P., 1996. "H_∞: design with pole placement constraints: an LMI approach". *IEEE Transactions on Automatic Control*, Vol. 41, No. 3, pp. 358–367. ISSN 0018-9286. doi:10.1109/9.486637.

Costa, T.L., Lara-Molina, F.A., Bolzon, V.R., Koroishi, E.H. and Colombo, D.A., 2016. "Identificação de parâmetros de um manipulador robótico utilizando o método dos mínimos quadrados". In *IX Congresso Nacional de Engenharia Mecânica - CONEM 2016*.

Florian, A., 1992. "An efficient sampling scheme: updated latin hypercube sampling". *Probabilistic engineering mechanics*, Vol. 7, No. 2, pp. 123–130.

Hunt, L., Su, R. and Meyer, G., 1983. "Global transformations of nonlinear systems". *IEEE Transactions on Automatic Control*, Vol. 28, No. 1, pp. 24–31.

Lara-Molina, F., Koroishi, E., Dumur, D. and Steffen, V., 2015. "Stochastic analysis of a 6-dof fully parallel robot under uncertain parameters". *IFAC-PapersOnLine*, Vol. 48, No. 19, pp. 214–219.

Lara-Molina, F.A., 2012. *Simulação e implementação experimental de um controlador preditivo generalizado para um robô orthoglide baseado na modelagem dinâmica*. Ph.D. thesis, Univesidade Estadual de Campinas.

Lara-Molina, F.A., Rosário, J.M., Dumur, D. and Wenger, P., 2014. "Robust generalized predictive control of the orthoglide robot". *Industrial Robot: An International Journal*, Vol. 41, No. 3, pp. 275 – 285.

Lewis, F.L., Dawson, D.M. and Abdallah, C.T., 2003. *Robot Manipulator Control: Theory and Practice*. CRC Press.

Lofberg, J., 2005. "YALMIP: A toolbox for modeling and optimization in MATLAB". In *Computer Aided Control Systems Design, 2004 IEEE International Symposium on*. IEEE, pp. 284–289.

Manesco, R.M. and P., S.J.H., 2012. "Estabilidade robusta h_∞ de sistemas lineares: uma implemetação em um helocóptero 3-dof de bancada". In *Anais do XIX Congresso Brasileiro de Automática, CBA 2012*.

Qu, Z. and Dawson, D.M., 1995. *Robust tracking control of robot manipulators*. IEEE press.

Sage, H., De Mathelin, M. and Ostertag, E., 1999. "Robust control of robot manipulators: a survey". *International Journal of control*, Vol. 72, No. 16, pp. 1498–1522.

Spong, M.W., 1992. "On the robust control of robot manipulators". *IEEE Transactions on automatic control*, Vol. 37, No. 11, pp. 1782–1786.

Wu, J., Wang, J. and You, Z., 2010. "An overview of dynamic parameter identification of robots". *Robotics and computer-integrated manufacturing*, Vol. 26, No. 5, pp. 414–419.

Zhou, K., Doyle, J.C., Glover, K. *et al.*, 1996. *Robust and optimal control*, Vol. 40. Prentice hall New Jersey.

10. RESPONSIBILITY NOTICE

The following text, properly adapted to the number of authors, must be included in the last section of the paper:
The author(s) is (are) the only responsible for the printed material included in this paper.